

# Adaptive GTS allocation scheme with applications for real-time Wireless Body Area Sensor Networks

**Xiaoli Zhang, Yongnu Jin, Kyung Sup Kwak\***

School of Information and Communication Engineering, Inha University,  
Incheon, Korea

[e-mail: hnyppy@gmail.com, grape412@163.com, kskwak@inha.ac.kr]

\*Corresponding author: Kyung Sup Kwak

*Received July 29, 2014; revised July 21, 2015; accepted March 20, 2015;  
published May 31, 2015*

---

## Abstract

The IEEE 802.15.4 standard not only provides a maximum of seven guaranteed time slots (GTSs) for allocation within a superframe to support time-critical traffic, but also achieves ultralow complexity, cost, and power in low-rate and short-distance wireless personal area networks (WPANs). Real-time wireless body area sensor networks (WBASNs), as a special purpose WPAN, can perfectly use the IEEE 802.15.4 standard for its wireless connection. In this paper, we propose an adaptive GTS allocation scheme for real-time WBASN data transmissions with different priorities in consideration of low latency, fairness, and bandwidth utilization. The proposed GTS allocation scheme combines a weight-based priority assignment algorithm with an innovative starvation avoidance scheme. Simulation results show that the proposed method significantly outperforms the existing GTS implementation for the traditional IEEE 802.15.4 in terms of average delay, contention free period bandwidth utilization, and fairness.

---

**Keywords:** IEEE 802.15.4, real-time, WBASN, Medium Access Control, GTS

---

This work was supported by National Research Foundation of Korea - Grant funded by the Korean Government (Ministry of Science, ICT and Future Planning)-NRF-2014K1A3A1A20034987) and by the MSIP(Ministry of Science, ICT and Future Planning), Korea, under the ITRC(Information Technology Research Center) support program (NIPA-2014-H0301-14-1042)'

## 1. Introduction

With recent improvement in system-on-chip designs, microelectronics and integrated circuits, wireless communication, and intelligent low-power sensors [1], wireless personal area networks (WPANs) are attracting increasing research attention from both academic and industrial areas. The wireless body area sensor network (WBASN) is a special WPAN with applications in health-care [2], military, sports training, and other value-added areas [3]. The main requirements of WBASNs are low-rate, short-distance, and low-cost. Among some well-known specifications, the IEEE 802.15.4 standard, which targets ultralow costs, complexity, and power for low-rate wireless connectivity among inexpensive portable moving devices [4], is recognized as one of the most promising options for the short-transmission-range WBASNs.

Fig. 1 shows a superframe structure adopted by the IEEE 802.15.4 beacon-enabled mode [5]. The protocol provides guarantees for real-time data transmission by utilizing the guaranteed time slot (GTS) mechanism in the contention free period (CFP) of the beacon-enabled mode. The GTS allocation is especially attractive for the applications in time-sensitive WBASNs because it can improve the reliability and performance of data transmissions due to scheduled transmissions. However, the fixed first-come first-served (FCFS) scheduling policy [5-6] may not satisfy the time constraints on time-sensitive transactions with delay deadlines very well, especially in medical and manufacturing sensor networks that monitor emergency events [7]. The issue is further exacerbated when the abuse of dedicated resources leads to the exclusion of other data deliveries and some devices are starved with low data transmission frequencies due to a fixed timer and an inflexible de-allocation problem [8-10].

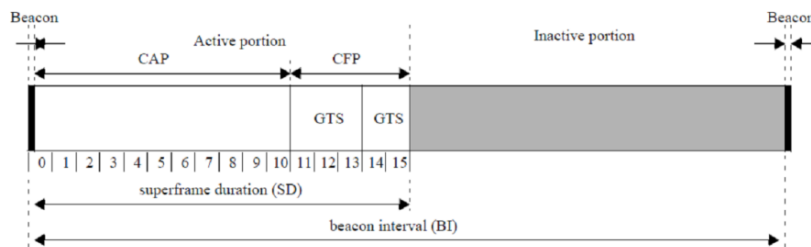


Fig. 1. Superframe structure for the IEEE 802.15.4 scheme.

Considerable research efforts have been recently devoted to evaluating the performance of both carrier sense multiple access with collision avoidance (CSMA/CA) and GTS mechanisms of the IEEE 802.15.4 protocol [14-17]. In [18], researchers proposed an implicit GTS allocation mechanism henceforth referred to as the iGAME algorithm. This algorithm not only supports higher bandwidth utilization, but also allows GTS sharing among many devices in a round-robin fashion. However, the iGAME does not guarantee delay requirements well and starvation is never addressed. In [19], an explicit GTS scheduling algorithm was proposed to guarantee the delay constraints in scenarios where all seven GTS slots were occupied by networked devices. However, this algorithm operated under too many constraints. In [20], an algorithm was developed called the earliest delay constraint with minimum GTS. This proposal dealt with assigning a minimum number of GTSs to as many transactions as possible in every beacon interval. Although it satisfied the delay-sensitive transactions well, it went

unmentioned how well it reduced GTS starvation leading to the possibility that the overhead required more energy consumption. Huang et al. [11] utilized a classification phase and a GTS scheduling phase in an AGA scheme. The main advantage to this algorithm is that it considers latency and fairness during GTS allocation. However, this proposal failed to consider any mechanism to improve the bandwidth utilization of GTS-allocated devices. Other protocols aiming at throughput improvement were presented in [21-23].

This paper focuses on the GTS allocation mechanism in IEEE 802.15.4 and without introducing any extra overhead proposes an adaptive GTS allocation scheme considering low latency and fairness [5]. In our proposed scheme, devices are divided into three traffic patterns and are followed the rule presented in a state transition diagram. For devices in normal traffic, differentiated services are provided and a weight-based priority assignment algorithm (WPAA) is designed. This WPAA assigns the priorities of devices in a dynamic fashion considering their recent GTS-usage feedbacks. In this way, devices that require more attention from the coordinator are assigned higher priority to access GTS resources. Additionally, we propose a clock-ring starvation avoidance mechanism (CRSAM) to manage lower priority devices, which are at risk of starvation due to insufficient GTSs for data transmissions over a long period. A careful performance evaluation of our proposed scheme is given by comparing it to the existing IEEE 802.15.4 MAC through simulations in terms of average packet delay, CFP bandwidth utilization, and fairness.

This paper is divided into four sections. In Section 2, we describe the basic principles of our proposed scheme. The mathematical analysis and simulation results are given in Section 3. Finally, Section 4 offers conclusions.

## 2. Adaptive GTS allocation scheme

The objective in this section is to present our basic principles and design algorithms for the IEEE 802.15.4-based WBASNS, considering low latency, bandwidth utilization, and fairness. A typical body area network (BAN) [12] consists of a number of inexpensive, lightweight, and miniature sensor platforms, each featuring one or more physiological sensors. These sensors can be located anywhere on the body as tiny intelligent patches, integrated into clothing, implanted below the skin, or deeply embedded in tissues. A typical BAN consists of a few devices (called BAN nodes or BNs) with the option to add more devices as required. The central device, called a BAN network controller (BNC or Hub), is used to manage and coordinate the BAN. Fig. 2 shows a typical BAN architecture.

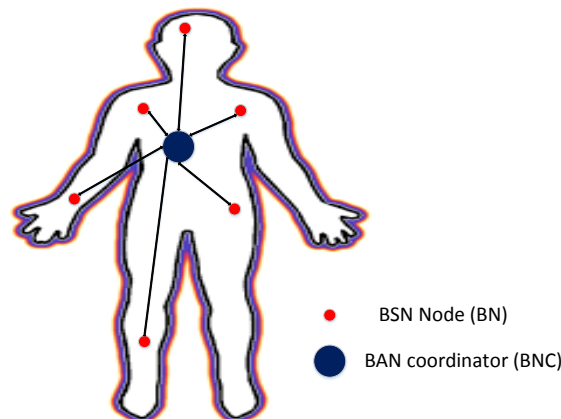


Fig. 2. Star-shaped topology of a BAN.

Data from these sensors is collected periodically. Emergency data, however, is generated suddenly and requires immediate transmission. Hence, relatively limited GTS resources should be assigned to needy devices with continuous data transmission. By contrast, previously allocated but unused GTSs should be reassigned in time.

For convenience, we define a CSMA/CA hit, a CSMA/CA miss, a GTS hit and a GTS miss as follows:

- ◆ CSMA/CA hit and CSMA/CA miss: A device is defined as having a CSMA/CA hit if it has attempted to access the channel in the CAP of the current superframe, regardless of whether the attempt had succeeded. Otherwise, the device is considered as having a CSMA/CA miss [10].
- ◆ GTS hit and GTS miss: Similarly, a device is defined as having a GTS hit if it has issued a successful GTS request in the CAP or if it has transmitted data within its allocated GTS to the PAN coordinator during the CFP period of the current superframe. Otherwise, the device is considered as having a GTS miss [11].

It is obvious that a CSMA/CA hit or a GTS hit represent more recent traffic for a certain device, whereas a CSMA/CA miss or a GTS miss indicate comparatively light traffic. Consequently, the recent data transmission behavior of devices can be well known through the occurrence of CSMA/CA hits/misses and GTS hits/misses. Here, we define ‘H’ to refer an event that CSMA/CA hit or GTS hit or both happen, while ‘M’ represents that both CSMA/CA miss and GTS miss happen. Therefore, ‘H’ is an union of CSMA/CA hit and GTS hit, and ‘M’ is an intersection of CSMA/CA miss and GTS miss as the following two equations.

$$H = \{H_{CSMA/CA} \cup H_{GTS}\} \quad (1)$$

$$M = \{M_{CSMA/CA} \cap M_{GTS}\} \quad (2)$$

where  $\cup$  is the union or sum logical operation and  $\cap$  is intersection or product logical operation. Since  $H_{CSMA/CA} = \overline{M_{CSMA/CA}}$  and  $H_{GTS} = \overline{M_{GTS}}$ , from (1) and (2), it can be easily proved that  $H = \overline{M}$ . In this way, the recent data transmission behavior of devices can be recorded by the coordinator and based on the previous and current transmission condition of a device, the following WPAA in the Section 2.3.1 can be applied.

### 2.1. Device Classification

Devices are classified into three traffic patterns: emergency, pseudo-emergency, and normal traffic. Furthermore, we rename a hit/miss (including both CSMA/CA hit/miss and GTS hit/miss) in emergency cases as E-hit/E-miss, and E'-hit/E'-miss in pseudo-emergency traffic. Accordingly, a hit/miss in normal traffic is represented by N-hit/N-miss.

Emergency traffic represents the highest priority level, bringing about an emergency message or an alarm. Such traffic is initiated by devices in the event of an emergency, and it is entirely unpredictable. When an emergency occurs, time-critical data is transmitted immediately, privileging it over the less-critical data.

Pseudo-emergency traffic is initiated by devices, which might be starved due to low data-transmission frequencies. In Section 2.3.2, we propose a CRSAM to prevent devices in light traffic from starvation. With the CRSAM, a parameter  $Q_n$  is defined to state the liveness of a device's clock. When  $Q_n$  reaches 0—that is, at the moment the clock

expires—the device will send this information to the coordinator and attempt to access the channel. Because this kind of traffic does not issue a real emergency event, the priority level is lower than that of actual emergency traffic but higher than that of normal traffic.

Normal traffic means that there are neither time restrictions for transmission nor exceptional phenomena for any data. Normal traffic patterns are initiated by devices under normal circumstances and send routine health information to the coordinator. This kind of traffic is generated heavily on a periodic basis and should be handled carefully.

## 2.2. State Transition

During the CAP, devices, which want to request new GTS allocations, send GTS request command to the BAN coordinator, and this request command changes the traffic pattern information. The state transition of devices with heterogeneous traffic patterns is scheduled as shown in Fig. 3, where emergency traffic, pseudo-emergency traffic, and normal traffic are represented by  $S^E$ ,  $S^{PE}$ , and  $S^N$ , respectively. Notably, a new state,  $S^0$ —an interim state between  $S^N$  and  $S^E$ —is introduced with some interesting properties. For example, devices residing in the  $S^E$  state with the occasional transmission interruption have a second chance before being downgraded to the normal traffic level state, at which temporarily unstable transmission device behavior is more tolerable.

The order of traffic levels for these states is  $S^E > S^{PE} > S^0 > S^N$ . Initially, all devices are placed in the  $S^N$  state. At the end of each superframe, the coordinator examines the GTS usage for all devices before deciding which state each device subsequently transitions toward. The transition follows the solid and dashed lines in Fig. 3. Solid lines represent the occurrence of a CSMA/CA or GTS hit, while dashed lines signify a CSMA/CA or GTS miss. In accordance with the rules in the state transition diagram, devices with more time-critical events are prioritized for data transmission.

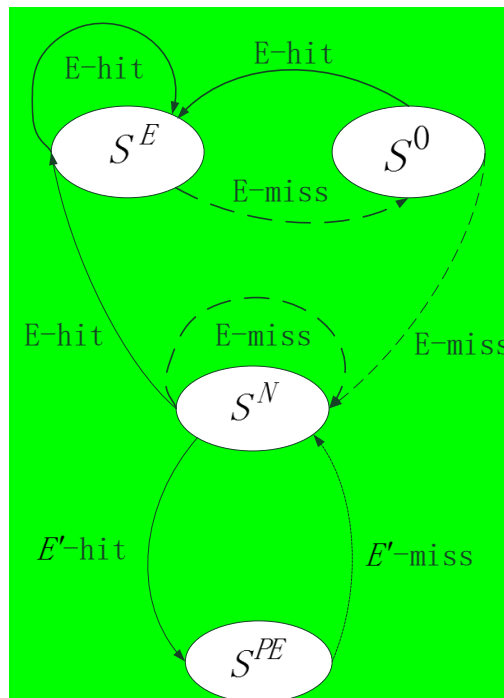


Fig. 3. State transition diagram.

The details for state and priority maintenance are described as follows:

- (a) Initially, all devices are placed in the  $S^N$  state, indicating that there are no exceptional events or real-time restrictions.
- (b) When an E-hit occurs—that is, when the device detects the setting for an exception or real-time restriction—the current state switches to  $S^E$  and reports an emergency message or alarm to the coordinator. Otherwise, the  $S^N$  state will be maintained.
- (c) Devices in the  $S^E$  state are sustained, provided that the E-hit is continually detected. However, whenever requirements for this particular state cannot be satisfied, the state will be set to  $S^0$ , meaning that its priority decreases.
- (d) When an exception is again detected or when a real-time restriction is reset, devices in the  $S^0$  state are upgraded to  $S^E$ . Otherwise, devices belonging to the  $S^0$  state are downgraded one level lower to  $S^N$  due to the occurrence of a consecutive E-miss.
- (e) Devices in the  $S^N$  state switch to  $S^{PE}$  provided that an  $E'$ -hit is detected. In other words, when the clock for a device in light traffic expires, the coordinator is notified to prevent device starvation. However, if a device in light traffic that has successfully maintained the  $S^{PE}$  state encounters an  $E'$ -miss, it will be demoted to  $S^N$ .

### 2.3. Service Differentiation

Generally, emergency data is generated with a small probability; while most data transmissions belong to normal traffic, and pseudo emergency traffic can be regarded as a special case of normal traffic. Therefore, the provided differentiated services are discussed as follows.

Emergency data transmissions are improbable, GTS resource allocation is comparatively sufficient for this kind of event. It has the highest priority level for GTS allocation.

For the devices in normal traffic, their recent data transmission behavior can be known through the occurrence of N-hits and N-misses. An N-hit represents more recent traffic for a certain device, while an N-miss indicates relatively light traffic. Therefore, priorities of normal traffic are set dynamically according to the transmission feedback. Our scheme provides a parent-child-based tree-structure algorithm for updating the priority numbers, named as the WPAA (described in the following section). Through the WPAA, we assign higher priority to devices with more recent traffic having a higher likelihood of transmitting data in the subsequent superframe.

Finally, for devices in pseudo-traffic, we propose a starvation avoidance mechanism to reestablish service attention to lower-priority devices. Details for this mechanism, known as the CRSAM, are provided in Section 2.3.2.

#### 2.3.1. A Weight-based Priority Assignment Algorithm

Although the coordinator can roughly monitor the recent transmission behavior of the devices, it is not effective given limited GTS resources (there are only seven). Thus, we propose a WPAA to dynamically assign the specific priority number to each device by the coordinator according to the recent transmission feedback. Hence, GTS resources can be allocated to more needy devices with consecutive transmissions.

Assume that device  $n$  maintains the following parameters at the beginning of the current

superframe.  $PRI_{n_{i-1}}$  and  $PRI_{n_i}$  are the weight-based priorities in depth  $(i-1)$  and in depth  $i$  of the tree structure (see Fig. 4), respectively. Provided that each device receives the beacon at the beginning of the current superframe, the weight-based priority of device  $n$ , i.e.,  $PRI_{n_i}$ , will be updated as follows:

$$PRI_{n_i} = PRI_{n_{i-1}} + W_{c_i} \quad (3)$$

$PRI_{n_0}$  can be obtained from past transmission feedback. Alternatively,  $PRI_{n_i}$  can be deduced from earlier  $PRI_{n_{i-1}}$  because a recursive sequence is implicit in the principle of mathematical induction [9].

$W_{c_i}$  is derived as follows:

$$W_{c_i} = \begin{cases} 2W_{p_i}, & c_{p_i} = c_{c_i} \\ -W_{p_i}, & c_{p_i} \neq c_{c_i} \end{cases} \quad (4)$$

where  $W_{p_i}$  and  $W_{c_i}$  are the nodes' weight values in depth  $i$  of the tree structure (see Fig. 4) under the previous and current condition, respectively.  $c_{p_i}$  and  $c_{c_i}$  are the previous and current condition mapped to a parent node and a child node (as in Fig. 4), respectively. In other words, the weight of a child node is twice that of its parent node if the current condition is the same as the previous condition (HH/MM). Otherwise (HM / MH), it is equivalent to its parent node's opposite number. Notice that  $|W_{p_i}| = |W_{c_i}| = 1$  is a given condition.

For example, consider  $PRI_{1_8} = PRI_{2_8} = 20$ ,  $c_{p_9} = H$  and  $W_{p_9} = +8$  for Device 1 and Device 2. Suppose there is an N-hit for Device 1 and an N-miss for Device 2 in the current superframe. Thus,  $c_{c_9} = H$  for Device 1, and  $c_{c_9} = M$  for Device 2. The weight-based priorities are obtained as follows:

$$PRI_{1_9} = PRI_{1_8} + W_{c_9} = PRI_{1_8} + 2W_{p_9} = 20 + 16 = 36 \quad (5)$$

$$PRI_{2_9} = PRI_{2_8} + W_{c_9} = PRI_{2_8} - W_{p_9} = 20 - 8 = 12. \quad (6)$$

In the above case, Device 1 and Device 2 have the same previous weight-based priority. When there is an N-hit/N-miss in the current superframe, the priorities for the two devices are changed to different values: (+16) for Device 1 in the case of an N-hit, and (-8) for Device 2 given an N-miss. The reason is that devices with continual N-hits, indicating consecutive transmissions, is given a higher priority, while devices with temporarily unstable transmission behavior, is assigned a lower priority.

Fig. 4 presents the tree structure for the WPAA process in a superframe. It is obvious that the devices with high-frequency sending are favored by our algorithm, while devices that are idle for a period of time will be downgraded dramatically by the coordinator, and the unused



GTS resources will be reclaimed immediately by the devices with heavy traffic. Therefore, with this approach, devices use GTS resources more efficiently.

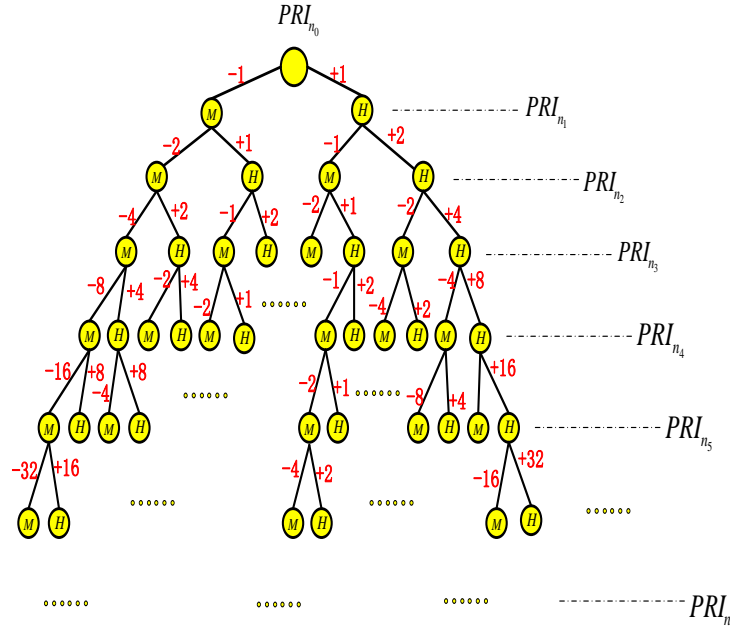


**Fig. 4.** Tree structure for the WPAA. For each node, the red numbers denote its weight value, and the yellow circles illustrates the condition of a certain device  $n$ , in which M/H represents an occurrence of an N-miss and an N-hit, respectively.

### 2.3.2. A Clock-Ring Starvation Avoidance Mechanism

By using the WPAA method, devices with more frequent data transmissions will have a higher probability of obtaining GTS allocation in the following superframe, while devices with relatively light recent traffic will be less likely to gain GTS resources. Although the effective utilization of GTSs is considerably improved, the starvation problem for devices with low traffic requires our urgent attention. To address this issue, we propose an innovative starvation avoidance scheme, named as CRSAM.

A device  $n$  maintains a table as follows:

$$NH_n \mid Q_n$$

where  $NH_n$  is the N-hit number for device  $n$  in the current superframe, and  $Q_n$  is a threshold value derived as follows:

$$Q_n = \left\lceil \frac{NH_{\max}}{NH_n} \right\rceil \tag{7}$$

where  $NH_{\max}$  is the N-hit number for the device with the highest priority. That is, it is the maximum value among all devices' N-hit numbers in the current superframe.

Algorithm 1 describes the design and implementation of the CRSAM. Whenever a change occurs on a certain device in low traffic, the value of  $Q_n$  changes correspondingly. Parameter



NC is TRUE if an N-hit occurs. Otherwise, NC is FALSE. If NC is TRUE, then  $NH_n$  increases by one and  $Q_n$  changes based on Formula (7). If NC is FALSE, then  $NH_n$  maintains the same value and  $Q_n$  is reduced by one. When the value of  $Q_n$  is below or equal to the normal boundary 0, the E'-hit will be initiated and the traffic state will follow the state transition diagram (described in Fig. 3).

---

**Algorithm 1.** A Clock-Ring Starvation Avoidance Algorithm

---

```

1:  while  $Q_n > 0$  do
2:    if NC = TRUE
3:       $NH_n = NH_n + 1$ 
4:       $Q_n = \left\lceil \frac{NH_{\max}}{NH_n} \right\rceil$ 
5:    else  $Q_n = Q_n - 1$ 
6:    end if
7:  end while
8:  E'-hit occurs
9:  Go into state transition diagram (Fig. 3)

```

---

As mentioned in Section 2.1, a device will not attempt to access the channel when  $Q_n$  is alive. However, the clock rings when  $Q_n$  reaches 0. By this method, the device reports the coordinator that it fails to access the channel for a relatively long period and wants to request GTS allocation. The coordinator then checks whether there are resources available in the current superframe for this pseudo-emergency because emergency events are given the highest priority. Under normal circumstances (that is, when the maximum length of seven time slots has not been reached), the device is momentarily provided with GTS allocation. Once the data transmission is completed, GTS resources are reallocated to high traffic devices. When resources are not available, the device must wait until the next superframe. Therefore, starvation can be avoided in low-priority devices with the CRSAM.

### 3. Performance Evaluations

#### 3.1. Mathematical Analysis

Traffic is modeled using a Poisson process with an arrival rate  $\lambda$  and a service rate  $\mu_s$  and a single queue with a finite buffer is employed. Additionally, a new packet is blocked if it finds that the queue is full. In this work, we assume that the offered load ( $\rho$ ) is less than one. Two traffic types generated by devices are considered: heavy traffic and light traffic.  $\lambda_h$  and  $\lambda_l$  represent the arrival rates for heavy-traffic and light-traffic devices, respectively. Let  $P_h$  denote the probability of heavy-traffic devices and  $P_l$  represent the probability of light-traffic devices. Hence, the arrival rate  $\lambda$  is given as:

$$\lambda = \lambda_h P_h + \lambda_l P_l \quad (8)$$

$$\frac{1}{\mu_s} = T_x + T_{ACK} \quad (9)$$

The term  $T_x$  is the time taken to transmit a packet of size  $x$ , and  $T_{ACK}$  is the time taken for the acknowledgement (ACK) transmission.

$$T_x = 8 \times \frac{L_{PHY} + L_{MAC\_HDR} + L_{address} + x + L_{MAC\_FTR}}{R} \quad (10)$$

where  $L_{PHY}$  is the length of the PHY header in bytes,  $L_{MAC\_HDR}$  is the length of the MAC header in bytes,  $L_{address}$  is the length of the MAC address,  $L_{MAC\_FTR}$  is the length of the MAC footer in bytes, and  $R$  is the raw data rate in bits per second (bps). Thus,  $T_{ACK}$  in (9) can be calculated as:

$$T_{ACK} = 8 \times \frac{L_{PHY} + L_{MAC\_HDR} + L_{MAC\_FTR}}{R} \quad (11)$$

The average delay for the traditional 802.15.4 MAC protocol ( $D_{15.4}$ ) and the proposed scheme ( $D_{ps}$ ) can be obtained from the following expressions:

$$D_{15.4} = W_q + T_{Beacon} + T_{BO} + 2T_{ACK} + T_x + T_{IFS} + T_{SD} \quad (12)$$

$$D_{ps} = W_q + T_{Beacon} + T_{BO} + T_{ps} + 2T_{ACK} + T_x + T_{IFS} \quad (13)$$

where  $W_q$  is the per-packet queue-waiting time in terms of the number of packets in the queue,  $T_{Beacon}$  is a beacon duration,  $T_{BO}$  is the duration of the back-off period,  $T_{IFS}$  is the general IFS time for packets of size  $x$ ,  $T_{SD}$  is a superframe duration, and  $T_{ps}$  is the time taken for priority assignment with the proposed scheme. Notice that a node performs a clear channel assessment (CCA) twice during the back-off procedure in the beacon-enabled IEEE 802.15.4. The back-off duration can thus be expressed as

$$T_{BO} = BO_{slots} \times T_{BO\_slot} + 2T_{CCA} \quad (14)$$

The term  $BO_{slots}$  refers to the average number of slots to which the node deferred its transmission.  $T_{BO\_slot}$  is the slot duration, and  $T_{CCA}$  is the time required for the CCA.

The per-packet queue-waiting time ( $W_q$ ) in terms of the number of packets in the queue can be calculated as

$$W_q = \frac{q_n}{\lambda(1-p_b)} \quad (15)$$

Let  $q_n$  be the number of packets in the queue, and  $p_b$  be the blocked probability. Additionally,  $k$  is the buffer capacity with a queue of  $k$  length packets. Obviously, the number

of packets in the queue affects the packet delay  $q_n$ , which is given by:

$$q_n = \frac{\rho}{1-\rho} - \frac{(k+2)\rho^{k+2}}{(1-\rho)^{k+2}} \quad (16)$$

The blocked probability ( $p_b$ ), the offered load ( $\rho$ ), and the queue utilization ( $\sigma_q$ ) are defined as follows:

$$p_b = \frac{(1-\rho)\rho^k}{1-\rho^{k+1}} \quad (17)$$

$$\rho = \lambda / \mu_s \quad (18)$$

$$\sigma_q = \rho(1-p_b) \quad (19)$$

We then calculate the throughput in terms of packets successfully delivered. The average throughput can be expressed as

$$S = \frac{\sigma_q}{\mu_s} \cdot x = \frac{\rho(1-p_b)}{\mu_s} \cdot x = \lambda(1-p_b) \cdot x \quad (20)$$

The CFP bandwidth utilization is obtained by:

$$BU = \lambda(1-p_b) \quad (21)$$

Furthermore, a fairness index  $F$  for the packet average delay is used to measure the fairness among different traffic-type devices for our scheme.  $F$  is defined in [13] as

$$F = \frac{(\sum_{i=1}^N D_i)^2}{\sum_{i=1}^N i \times D_i^2} \quad (22)$$

where  $N$  is the total number of devices in the network and  $D_i$  is the average packet delay for the packets generated by device  $i$ .

### 3.2. Simulation Setup

We considered two scenarios, with 10 nodes and 20 nodes are firmly fixed on a human body. The nodes are connected to the coordinator in a star topology and only uplink traffic is considered. Generally, the packet inter-arrival period,  $L_D$ —in normal traffic is constant. For emergency and pseudo-emergency traffic, by contrast, the packet inter-arrival period,  $L_p$ ,

follows an exponential distribution ( $1/L_p$  follows the Poisson distribution). In the simulation, each node has two traffic generators—i.e., a Poisson (emergency and pseudo-emergency) traffic generator, and a Deterministic (normal) traffic generator, where one generator can be used at a time according to the traffic pattern. The Poisson and deterministic traffics are generated from the following equations:

$$L_p = -\frac{1}{\lambda} \ln(1-p) \quad \text{with} \quad 0 \leq p \leq 1 \quad (23)$$

where  $p$  represents the probability, which is uniformly distributed in the interval  $[0, 1]$ .

$$R_N = a + [p(b-a) + 1] \quad \text{with} \quad (24)$$

$$0 \leq p(b-a) \leq 1, b > a$$

$$L_D = i \times R_N \quad (25)$$

First, a uniform generator is used to calculate a random number  $R_N$ , then  $L_D$  is generated ( $i$  times) as a function of  $R_N$ . Generally, each node has a unique  $R_N$ , and thus a different  $L_D$ .

Our simulations are based on the parameters shown in **Table 1**.

**Table 1.** Simulation parameters

Parameters	Values
Transmission Rate (R)	250 kbps
Synchronization Mode	Beacon enabled
Network Topology	Star topology
Number of Devices	10 and 20
$P_T$	27 mW
$P_R$	1.8 mW
$L_{PHY}$	6 Bytes
$L_{MAC\_HDR}$	3 Bytes
$L_{MAC\_FTR}$	2 Bytes
$L_{address}$	2 Bytes
Packet size (x)	1~10000 Bytes
$T_{CCA}$	8 Symbols
$T_{BO\_slot}$	20 Symbols
$T_{Beacon}$	80 Symbols
$BO_{slots}$	4
Superframe duration (SD)	7680 Symbols
$T_{IFS}$	12 /40 Symbols
$T_{ps}$	12 Symbols
Beacon Order (BO)	4
Superframe Order (SO)	3

The simulation flow diagram for the coordinator is depicted in Fig. 6, where the simulation flow chart of emergency response (ER) and pseudo-emergency response (PER) are drawn in Fig. 7 and Fig. 8, respectively. For normal traffic, the coordinator checks the traffic pattern and decides which node to transmit. If more than one node has the same traffic pattern, but with different priorities, resources are allocated to a high-priority node. However, if more than one node has the same traffic pattern as well as the same priority, then resources are allocated to a node having the maximum data volume. The remaining nodes wait until the high priority nodes complete their transmission and are subsequently served based on their priorities. For pseudo-emergency traffic, the coordinator first checks whether any emergency interrupts. If no emergency interrupts, resources are then the coordinator will check the available GTS numbers. If there are sufficient GTS resource, the resources are allocated to the nodes. Otherwise, the nodes wait until the emergency event is handled or the sources are available. Emergency traffic is generally considered to interrupt the normal operation of the coordinator. All processes cease when an emergency event occurs, and resources will be reallocated to the emergency node.

We run the simulation 100 times and the averaged values are recorded.

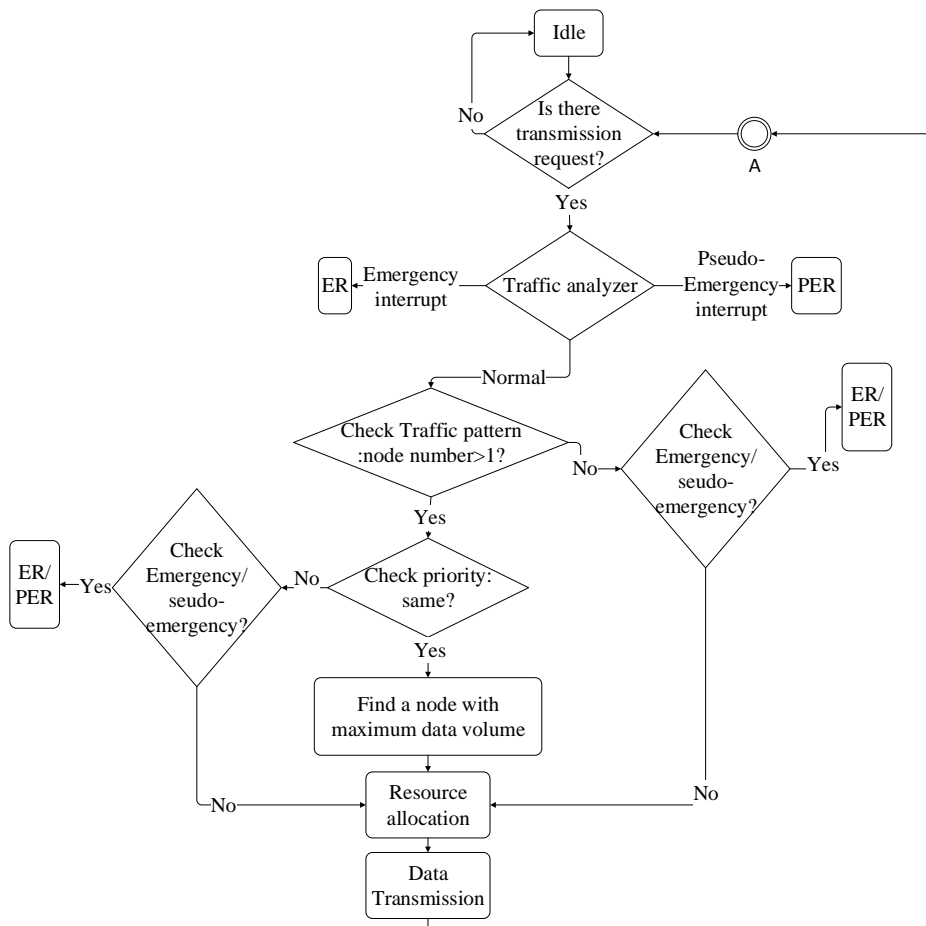


Fig. 6. Simulation flowchart for the coordinator.

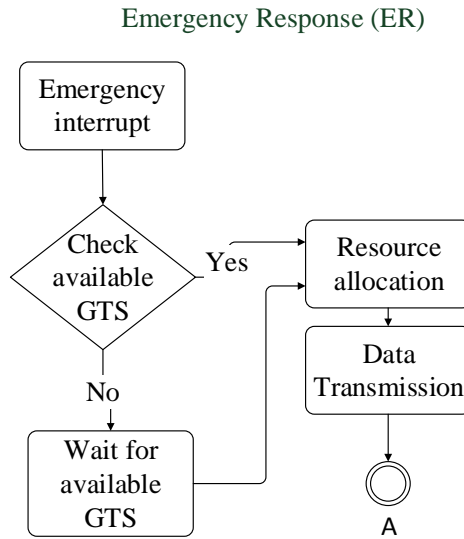


Fig. 7. Simulation flowchart of Emergency response

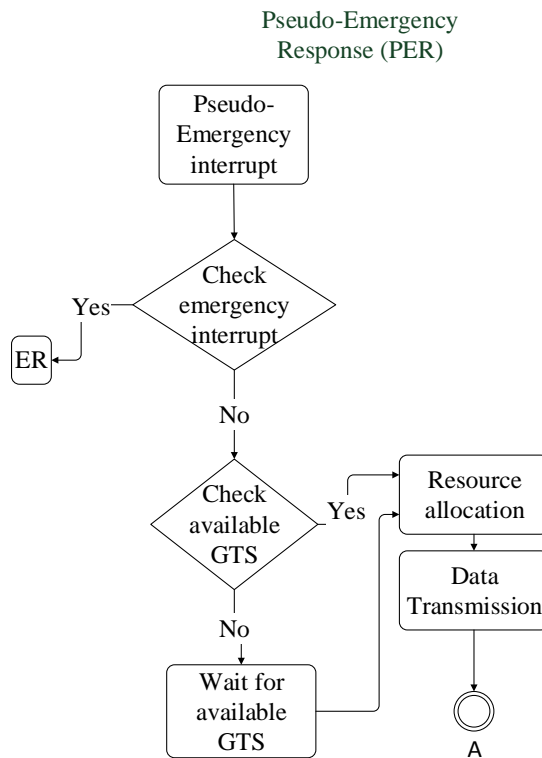
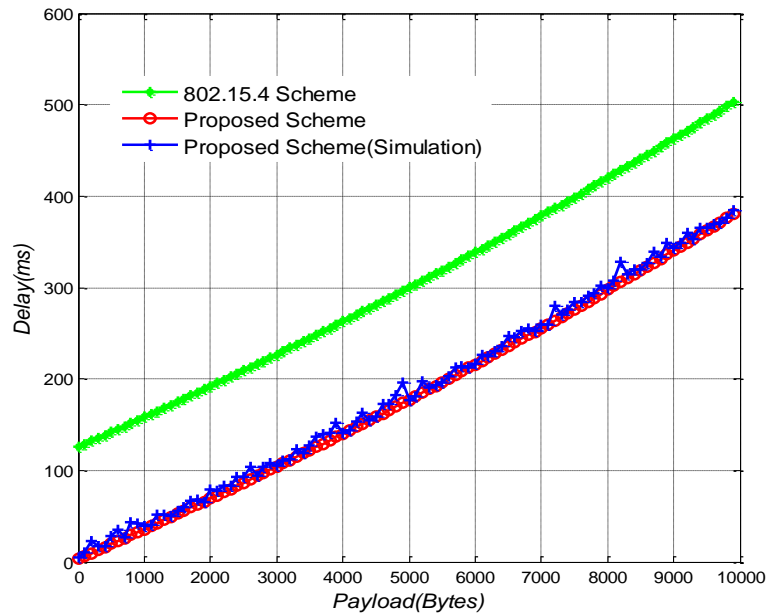


Fig. 8. Simulation flowchart of Pseudo-emergency response.

### 3.3. Simulation Results

**Fig. 9** illustrates the effect of the GTS data payload with an average delay—the green, red, and blue lines representing the conventional 802.15.4 scheme, our proposed scheme, and the simulation results for our proposed scheme, respectively. We observe that the average delay for the proposed scheme is far less than that of the 802.15.4 scheme, regardless of the payload size. The average packet delay increases as the payload size increases. The reason is that a bigger payload size requires more time for data transmission under both schemes. Furthermore, we observe that the proposed scheme performs adequately with an average delay for all payload sizes under investigation. Compared with the traditional 802.15.4 scheme, our scheme improves by approximately 120 ms. Since the proposed scheme meets the delay requirement well, the proposed scheme is much more favorable for WBASN time-sensitive applications.



**Fig. 9.** Effect of the payload with an average delay.

Our evaluation of GTS bandwidth utilization is also considered between the original 802.15.4 scheme and the proposed scheme under different traffic loads. From **Fig. 10**, we can see that the bandwidth utilization for both schemes increases as the packet payload increases in both low- and high-traffic environments. Because each device makes use of a higher proportion of the available GTS resources, and this makes the CFP bandwidth utilization correspondingly improved. Our proposed scheme increases sharply when the payload size is small. The main reason for this is that our proposed scheme incurs only some overhead before increasing slightly as the payload size becomes large. Under the 802.15.4 scheme, bandwidth utilization increases in small iterations as the payload size grows, where the overhead takes up a large proportion. Additionally, both schemes perform better in heavy traffic than in light traffic, because the unused GTSs are efficiently allocated to the devices, which are high-frequency transmitting. In general, CFP bandwidth utilization for our proposed scheme outperforms that of the traditional 802.15.4 scheme by 6% –28% in both light traffic and heavy traffic of all payload sizes.



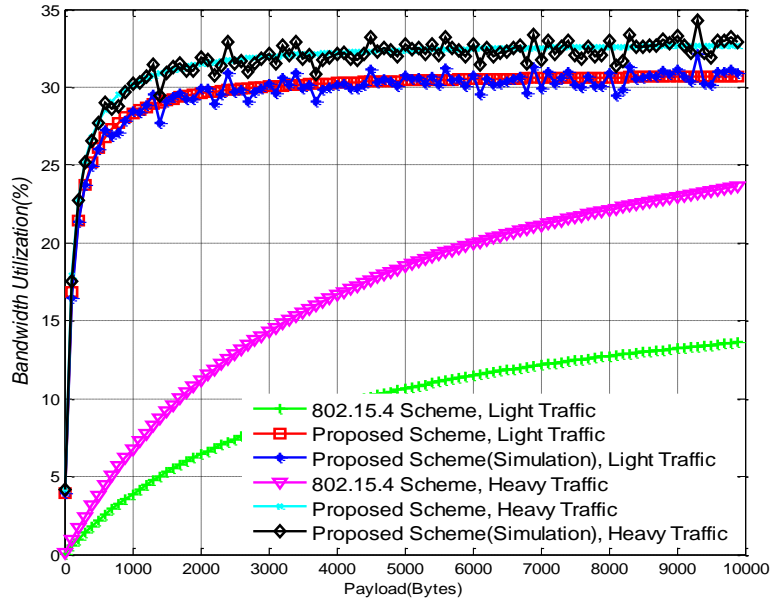


Fig. 10. Effect of the payload on CFP bandwidth utilization with different traffic loads.

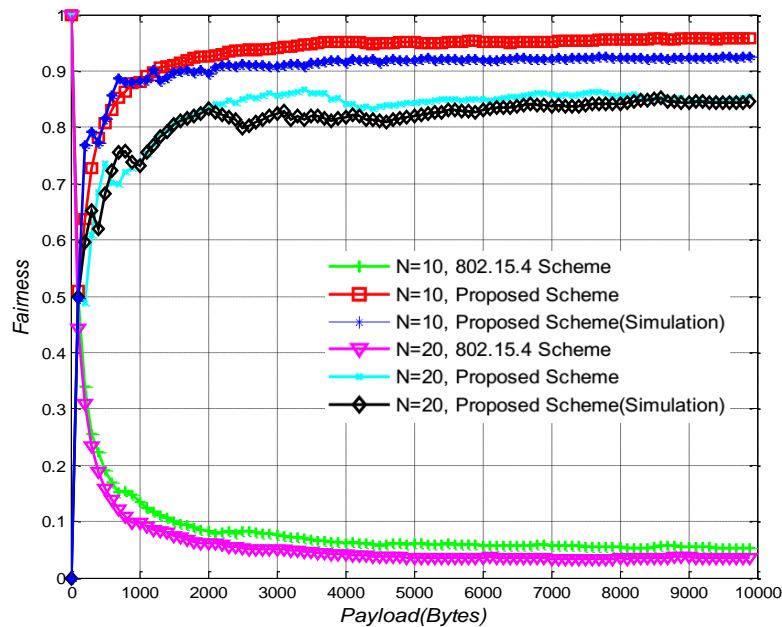


Fig. 11. Effect of the payload on fairness with different numbers of nodes.

Based on Formula (22), it is clear that  $0 \leq F \leq 1$ , and the effect of the packet payload on the fairness of GTS resource allocation for both our proposed scheme and the conventional 802.15.4 scheme is illustrated in Fig. 11. We observed that the experimental results for the proposed scheme are superior to those of the traditional IEEE 802.15.4 for most curves,

regardless how many devices are tested ( $N=10$  or  $N=20$ ). When the payload size becomes very large, we can achieve around 80% enhancement in terms of fairness. Note that  $F$  decreases as the payload increases under the conventional 802.15.4 scheme, implying that the inflexible FCFS policy aggravates the unfair situation when workload becomes heavy. However, the fairness of our proposed scheme increases as the payload goes up due to the flexibility of our scheduling policy. That is, our proposed scheme is equipped with the capacity to provide fairer transmissions among different kinds of devices.

#### 4. Conclusion

We have proposed an adaptive and real-time GTS-allocation scheme for WBASNs to improve the performance of the GTS mechanism for IEEE 802.15.4 WBANs in beacon-enabled mode. First, devices are classified into three distinct traffic patterns and strictly follow the rules developed in the state transition diagram. Based on the proposed WPAA, devices in normal traffic are dynamically assigned priority and provided with services. Devices in pseudo-emergency traffic are provided services by using a CRSAM that prevents the starvation of such devices in light traffic. Our scheme has been designed according to the existing IEEE 802.15.4 MAC protocol, with which IEEE 802.15.4 devices can implement the service without modification. Performance evaluations have been conducted through mathematical analysis and the experimental simulations. The simulations have demonstrated that our proposed scheme offers a significant improvement to network performance in terms of average delay, CFP bandwidth utilization, and fairness.

It is worth exploring how our proposed scheme performs in a real scenario applied to a working system. We are planning to apply the mechanism to a specific healthcare system and test its performance. Furthermore, additional quantitative comparisons with existing approaches are essential, and we fully intend to pursue this objective.

#### References

- [1] S. Ullah, H. Higgins, B. Braem et al., "A comprehensive survey of wireless body area networks—on PHY, MAC, and network layers solutions," *Journal of Medical Systems*, vol. 36, no. 3, pp. 1065–1094, 2012. [Article \(CrossRef Link\)](#).
- [2] M. Patel, and J. Wang, "Applications, challenges, and prospective in emerging body area networking technologies," *IEEE Wireless Communication Magazine*, vol. 17, no. 1, pp. 80-88, 2010. [Article \(CrossRef Link\)](#).
- [3] M. Chen, S. Gonzalez, A. Vasilakos, H. Cao, and V. C. M. Leung, "Body Area Networks: A Survey," *Journal of SPECIAL ISSUES on Mobility of Systems, Users, Data and Computing*, vol. 16, no. 2, pp. 171-193, 2011. [Article \(CrossRef Link\)](#).
- [4] E. Callaway, P. Gorday, and L. Hester, "Home Networking with IEEE 802.15.4: A Developing Standard for Low-Rate Wireless Personal Area Networks," *IEEE Communication Magazine*, Aug. 2002. [Article \(CrossRef Link\)](#).
- [5] IEEE Standard for Information Technology Part 15.4: Wireless Medium Access Control (MAC) and Physical Layer (PHY) Specifications for Low-Rate Wireless Personal Area Networks (LR-WPANs), *IEEE Standard 802.15.4 Working Group Standards*, 2007. [Article \(CrossRef Link\)](#).
- [6] A. Koubaa, M. Alves, and E. Tovar, "Time-Sensitive IEEE 802.15.4 Protocol," *chapter of the book: Sensor Networks and Configurations: Fundamentals, Techniques, Platforms, and Experiments*, Springer-Verlag, 2007. [Article \(CrossRef Link\)](#).
- [7] A. Koubaa, M. Alves, and E. Tovar, "GTS allocation analysis in IEEE 802.15.4 for real-time

- wireless sensor networks,” in *Proc. of International Parallel and Distributed Processing Symposium*, pp. 25–29, 2006. [Article \(CrossRef Link\)](#)
- [8] P. Park, C. Fischione, and K. H. Johansson, “Performance analysis of GTS allocation in beacon enabled IEEE 802.15.4,” in *Proc of 6th Annual IEEE Communications Society Conference on Sensor, Mesh and Ad Hoc Communications and Networks*, pp. 1–9, 2009. [Article \(CrossRef Link\)](#)
- [9] S. Wolfram, “Recursive Sequences, A New Kind of Science. Champaign,” *IL: Wolfram Media*, pp. 128-131 and 890-891, 2002. [Article \(CrossRef Link\)](#)
- [10] Y. Huang, A. Pang, and H. Hung, “An adaptive GTS allocation scheme for IEEE 802.15.4,” *IEEE Transactions on Parallel and Distributed Systems*, vol. 19, no. 5, pp. 641–651, 2008. [Article \(CrossRef Link\)](#)
- [11] F. Xia, R. Hao, J. Li et al., “Adaptive GTS allocation in IEEE 802.15.4 for real-time wireless sensor networks,” *Journal of Systems Architecture*, vol. 59, no. 10, pp. 1231-1242, 2013. [Article \(CrossRef Link\)](#)
- [12] B. Latre, B. Braem, I. Moerman et al., “A Survey on Wireless Body Area Networks,” *Journal of Wireless Networks*, vol. 17, no. 1, pp. 1-18, 2011. [Article \(CrossRef Link\)](#)
- [13] R.K. Jain, D.W. Chiu, and W.R. Hawe, “A Quantitative Measure of Fairness and Discrimination for Resource Allocation in Shared Computer Systems,” *DEC Technical Report TR-301*, 1984. [Article \(CrossRef Link\)](#)
- [14] C. Li, H. B. Li, and R. Kohno, “Performance evaluation of IEEE 802.15.4 for wireless body area network,” in *Proc. of IEEE International Conference on ICC Workshops*, pp. 1–5, 2009. [Article \(CrossRef Link\)](#)
- [15] N. F. Timmons, and W. G. Scanlon, “Analysis of the performance of IEEE 802.15.4 for medical sensor body area networking,” in *Proc. of IEEE SECON*, pp. 4–7, 2004. [Article \(CrossRef Link\)](#)
- [16] S. Ullah, H. Higgins, B. Shen, and K. S. Kwak, “On the implant communication and MAC protocols for WBAN,” *International Journal of Communication Systems*, vol. 23, no. 8, pp. 982-999, 2010. [Article \(CrossRef Link\)](#)
- [17] H. Li, and J. Tan, “An ultra-low-power medium access control protocol for body sensor network,” in *Proc. of 27th Annual International Conference of the Engineering in Medicine and Biology Society*, pp. 2451–2454, 2005. [Article \(CrossRef Link\)](#)
- [18] A. Koubaa, M. Alves, and E. Tovar, “i-GAME: an implicit GTS allocation mechanism in IEEE 802.15.4 for time-sensitive wireless sensor networks”, in *Proc. of 18th IEEE Euromicro Conference on Real-Time Systems*, pp. 169-204, 2006. [Article \(CrossRef Link\)](#)
- [19] J. Chen, L. Ferreira and E. Tovar, “An Explicit GTS Allocation Algorithm for IEEE 802.15.4”, in *Proc. of IEEE 16th Conference on Emerging Technologies & Factory Automation (ETFA)*, pp. 1-8, 2011. [Article \(CrossRef Link\)](#)
- [20] C. W. Na, “IEEE 802.15.4 Wireless Sensor Networks: GTS Scheduling and Service Differentiation”, 2011. [Article \(CrossRef Link\)](#)
- [21] L. Cheng, A.G. Bourgeois, and X. Zhang, “A new GTS allocation scheme for IEEE 802.15.4 networks with improved bandwidth utilization,” in *Proc. of International Symposium on Communications and Information Technologies*, pp. 1143-1148, 2007. [Article \(CrossRef Link\)](#)
- [22] C. L. Ho, C. H. Lin, W. S. Hwang, and S. M. Chung, “Dynamic GTS Allocation Scheme in IEEE 802.15.4 by Multi-Factor,” in *Proc. of Eighth International Conference on Intelligent Information Hiding and Multimedia Signal Processing (IHMSP)*, pp.457-460, 2012. [Article \(CrossRef Link\)](#)
- [23] C. Huang, H. W. Wu, and Y. W. Lee, “A Cluster Tree-Based GTS Allocation Scheme for IEEE 802.15.4 MAC Layer,” in *Proc. of Sixth International Conference on Innovative Mobile and Internet Services in Ubiquitous Computing*, pp. 524-528, 2012. [Article \(CrossRef Link\)](#)



**Xiaoli Zhang** completed her B.S. degree at Xidian University in 2012. From September 2012 to August 2014, she was involved in the M.S. program at the UWB Wireless Communications Research Lab, Inha University, Korea. Her research interests include multiple access communication systems and wireless body area networks.



**Yongnu Jing** received a B.S. degree from Chengdu University of Technology (CDUT) in 2002, an M.S. degree from the University of Electronic Science and Technology of China (UESTC) in 2006, and a Ph. D. degree from the Inha University, Incheon Korea in 2014. From 2006 to 2008, as a hardware engineer, she worked successively at O2Micro Co., Ltd and Conexant Digital TV Co., Ltd. She is currently working as a postdoctoral fellow at Inha University (under the supervision of Prof. Kyung Sup Kwak). Her research interests include UWB pulse shaping, multi-access interference (MAI) suppression, non-coherent receivers, wireless sensor networks, and intra-vehicle wireless communication application.



**Kyung Sup Kwak** received the Ph.D. degree from the University of California at San Diego in 1988. He had worked for Hughes Network Systems, California, USA and IBM Network Analysis Center, North Carolina, USA, and is now with Inha University, Korea as Inha fellow professor. He is directors of UWB Wireless Communications Research Center, Korea. He served as the president of Korean Institute of Information and Communication Sciences in 2006, and the president of Korea Institute of Intelligent Transport Systems in 2009. His research interests include multiple access communication systems, UWB radio systems and wireless sensor networks.